Istraživanja i projektovanja za privredu
ISSN 1451-4117
DOI:10.5937/jaes0-51363
www.engineeringscience.rs

iipp publishing

Journal of Applied Engineering Science
Vol. 22, No. 4, 2024
Original Scientific Paper
Paper number: 22(2024)4, 1238, 746-760

CFD INVESTIGATION OF THE EFFECT OF MODIFIED TWISTED TAPE ON HYDROTHERMAL ENHANCEMENT IN VERTICAL PIPE

Fawzi Sh. Alnasur [1,2] *, Riyadh S. Alturaihi [2]

[1] Al-Qadisiyah University, College of Science, Environmental Research Unit, Iraq
[2] University of Babylon, College of Engineering, Department of Mechanics, Iraq
** fawzi.shnain@qu.edu.iq*

Heat transfer enhancement has been a significant focus in hydrothermal engineering for several decades. The current paper represents an investigation using computational fluid dynamics (CFD) for a vertical circular tube having twisted taper inserted (plain and modified) with different twisted tape ratios TR, i.e., 7.8, 3.9, and 2.6, at three uniform wall heat fluxes and ranges of Reynolds number as boundary conditions. The twisted strips were used as a system to produce a turbulent, powerful swirl flow with an increase in the intensity of the secondary flow at the radial direction of the tube. The (friction facto) f and (Nusselt number) Nu were two measures of pressure loss and heat transfer variation that have been studied and graphically depicted. So, to balance the heat transfer enhancement quantity with pressure losses, the performance evaluation factor PEF was tested. It was observed that the twisted tape insert enhances the radial secondary flow intensity. The findings demonstrated that, in every scenario, the increase in(Reynold number)Re at the inlet, heat flux quantity, and twisted ratio results from a proportionate increase in heat transfer. At the same time, the friction factor decreases with an increase in all boundary conditions, except the twisted ratio, where the friction factor increases with increasing heat transfer. After accounting for heat transfer and friction coefficient, it was discovered that the tube with modified twisted stripe and the twist ratio was 3.9 performs best out of all the configurations examined. The performance evaluation factor PEF of pipes inserted with modified twisted tape was higher, reaching 1.5. This study is based on enhancing a high-performance evaluation factor of heat exchangers for use in industrial settings.

Keywords: twisted tape, swirling flow, performance evaluation factor

1 INTRODUCTION

Enhancement of convective heat transfer in various heat exchanger types can result in improved heat exchanger performance, which will lower the system's size and cost [1], which is used in numerous industries and engineering systems, including solar systems, fuel cells, air conditioning equipment, thermoelectric cooling, heat sinks, etc. [2-3]. These approaches are implemented in natural and forced convection heat transfer [4-6]. Different techniques enhance and improve heat transfer, such as fluted, different fines, micro-fined, louvered, wire brushes, coiled wires, and twisted-tape inserts [7-8]. The twisted tape inserts in the pipes are widely employed to enhance heat transfer in heat exchangers. Using the CFD method can be informative in studying the flow behavior of internal flows, which are difficult to obtain through traditional experimental tests. Different studies have been conducted to achieve optimal design and heat transfer performance [9]. Kim Leong Liaw et al. created a three-dimensional computational fluid dynamic model [10] to investigate the heat transfer enhancement in a turbulent flow constant wall temperature with a twisted tape core inserted in a helical tube. Convective heat transfer through straight tubes and coiled pipes with and without spiral band liners is assessed using correlations and experimental data. The twist ratio achieved the best performance at TR = 7.86, increasing in Nu proportionately, while the friction factor f decreased. The study by Ahmed Ramadhan Al-Obaidi et al. [11] aimed to numerically analyze the heat transfer enhancement and water flow characteristics. The three-dimensional numerical model was created with a straight tube using D (diameter) = 11 mm and the L(length) = 1920 mm, along with four twisted tapes with varying widths (1, 2, 2.5, and 3 mm) and twisted ribbon inserted with Re No. of (1500–24,000). The turbulent flow was demonstrated to be more prominent in a wider geometry of a twisted tape 1x3 mm. Using an insertion increased the losses in pressure in a tube. For twist strap inserts, improvements varied from 23% to 29%; inserting the wider twist tape saw greater enhancements. Using nanofluid (Al2O3/water), multi-semi-twisted tape inserts inside a heat exchanger pipe were studied hydrothermally numerically by Yongfeng Ju et al. [12]. When semi-twisted stripes numbers are raised from (0) to (4) with Re 1000, the Nu increases from 15.13 to 28.42, and the average enhancement of the friction factor was (0.022 - 0.052). Conversely, when Re increases from 250 to 1000, the friction factor minimizes from 0.155 to 0.052, and the Nu increases from 12.5 to 28.5 when four semi-twisted tapes are used. Using 4 semi-twisted tape, φ = 0.03 and Re= 750 achieved the highest performance evaluation criterion (PEC) of 1.66. The effect of thread pitch on hydrothermal performance when a stationary or rotating twisted ribbon is inserted into a pipe was evaluated numerically using simulations by Arasteh Hossein et al. [13]. Pitch reduction raises the Nu and friction coefficients in steady-state conditions. Nu, as well as the coefficient of friction, increases as the twisted tape begins to rotate (RTT1 scenario). Spinning the twisted ribbon at a lower Re was beneficial, according to Performance Evaluation Criteria. When the twist bandgap is L/6, and the fixed twist band is Re (1000), the maximum PEC of 1.5 is achieved. A unique correlation was discovered for a circular pipe with several short-length ribbons inserted with length ratio (LR=0.29,0.43,0.57, and1), constant heat flux by Anil Singh Yadav et al. [14] (CFD). The findings demonstrate that The SLTT for LR =

0.29, 0.43, and 0.57 has higher Nu at 1.07, 1.13, and 1.17 times, as well as higher friction losses of 1.78, 1.90, and 2.02 times compared to the smooth tube. Characteristics of heat transfer pressure drop and performance evaluation criteria (PEC) by the CFD with Re (100 - 1100) were investigated numerically by using conventional twisted tapes (TT) and new coaxial cross-twisted tapes (CCTTs) installed in the tube with molten salt FLiBe by Zimu Yang et al. [15] a fluid using were lubricating oil as well as water. According to findings, FLiBe employing CCTTs with high Prandtl numbers has the largest PEC, which was 2.37. In order to investigate the properties of heat transfer and the friction coefficient of fluid flowing into heat exchanger tubes equipped with double-cut twisted (DCT) using different cut ratios, M.E. Nakhchi et al. [16] conducted an experimental study with water serving as the working fluid and turbulent flow conditions (5000≤ Re ≤ 15,000), the rectangular cut ratio measured 0.25–0.90. The findings indicate that the increasing in the Nu was 177.4% when increased the cut ratio of 0.240 to 0.90. For the cut ratio of 0.90, the thermal performance ranges from 1.63 to 1.44 using the RNG k-ε turbulence model. The effects of the new conical twisted structure on the thermal and hydrodynamic fields in a heating tube with constant heat flux and air as the working medium with turbulence (10,000 ≤ Re ≤ 40,000) were investigated experimentally and numerically by Khudheyer S. Mushateta et al. [17]. For Nu, the maximum increase observed experimentally and numerically was 75% and 100%, respectively; for the friction factor, it was 220% and 226%, and for the thermal performance factor, it was 1.19 and 1.37M.EUsing an RNG k-ε model with Re =5000 to 1600, Nakhchi et al. [18] employed single-cut as well as double-cut techniques. Using different cut ratios (0.75 > b/w > 0.25 and 1 > c/w > 0.25), they numerically analyzed in three dimensions the thermal-hydraulic performance and flow structure for turbulent flow across pipe with twisted tape having rectangular cut. For b/w ≈0.75, the single-cut twisted stripe had a better thermal performance factor (1.21 - 1.65). N.T. Ravi Kumara et al. [19] conducted an experimental investigation into the convective heat transfer and friction losses of Fe3O4/water nanofluid flow through a double pipe U-bend using twisted tape with Re (16,000 to 32,000). The twisted tapes had φ of (0.0050% to 0.060%) and H/D ratios (20, 15, and 10). A friction coefficient reaches 1.25 times (with tapes having H/D = 10) and 1.1 times (without tape), while the Nu number increased by 14.76% (without insert) and rose to 38.70 % (using twisted ribbon, H/D ratio was 10, φ was 0.0610%, and the Re was (30,000). Numerical simulations of swirling flow brought on by a new coaxial cross-twisted tape in a heated pipe filled with lubricating oil were presented by Xiaoya Liu et al. [20], with (0) clearance ratios. The findings show that the coaxial cross-twisted ribbon' enhancements in heat transfer performance were better than a standard twisted tape when the clearance ratio was 0.077. When Re was between 200 and 1300, the maximum (PEC) reached (2.3.077, 0.154, and 0.231) when using TR of 2.4 at constant wall temperature conditions. The enhancement of heat transfer in tubes with multiple twisted ribbon inserts was experimentally investigated by S. Eiamsa et al. [22]. The contravertebral ligament (CT) and the converters ligament (CoT) were the alignments, and the twisters number (N) were (6, 4, and 2). The twisted ratios were 6, 5, and 4. Whenever air is utilized as the working fluid, the heat flow remains constant. It was demonstrated that the greater thermodynamic performance was 1.33 obtained when the Re (6000), TR (4.0) and N (6).

As we can see from the above, using twisted tape as a powerful vortex generator was crucial to boosting the flow inside the pipes' efficiency. The primary goal of this research is to confirm numerically the hydraulic (pressure drop) ΔP and thermal (heat transfer) characteristics of the three-dimensional vertical flow. This type of twisted tape (regular wavy edge) is considered a new update in the form of rigging tapes that affect the efficiency of pipes containing a modified twisted strip with three different twisting ratios (7.8,3.9 and 2.6) for three different flow speeds and three different heat flux which have not been considered before. The results can benefit the engineers in the design and selection of heat exchangers or any thermal system.

2 METHODOLOGY

2.1 Assumptions

It has been assumed that the fluid flow was turbulent, steady, and incompressible to resolve the governing equations. Ignore the radiation-induced heat transfer and the resistance to thermal contact between components and ignore viscous dissipation

2.2 Governing Equations

The governing equations for mass (continuity), momentum (in three dimensions), and energy were based on the abovementioned hypotheses. [24]:

Continuity equation:

$$\frac{\partial u}{\partial x}+\frac{\partial v}{\partial y}+\frac{\partial w}{\partial z}=0 \quad (1)$$

a) Momentum equations in 3-D (x,y,z)

In X-D
$$u\frac{\partial u}{\partial x}+v\frac{\partial u}{\partial y}+w\frac{\partial u}{\partial z}=-\frac{1}{\rho}\frac{\partial p}{\partial x}+\frac{\mu}{\rho}\left(\frac{\partial^2 u}{\partial x^2}+\frac{\partial^2 u}{\partial y^2}+\frac{\partial^2 u}{\partial z^2}\right) \quad (2)$$

In Y-D
$$u\frac{\partial v}{\partial x}+v\frac{\partial v}{\partial y}+w\frac{\partial v}{\partial z}=-\frac{1}{\rho}\frac{\partial p}{\partial y}+\frac{\mu}{\rho}\left(\frac{\partial^2 v}{\partial x^2}+\frac{\partial^2 v}{\partial y^2}+\frac{\partial^2 v}{\partial z^2}\right) \quad (3)$$

In Z-D $$u\frac{\partial w}{\partial x}+v\frac{\partial w}{\partial y}+w\frac{\partial w}{\partial z}=-\frac{1}{\rho}\frac{\partial p}{\partial z}+\frac{\mu}{\rho}\left(\frac{\partial^2 w}{\partial x^2}+\frac{\partial^2 w}{\partial y^2}+\frac{\partial^2 w}{\partial z^2}\right) \quad (4)$$

b) Energy equation

$$u\frac{\partial T_f}{\partial x}+v\frac{\partial T_f}{\partial y}+w\frac{\partial T_f}{\partial z}=\frac{k}{\rho cp}\left(\frac{\partial^2 T_f}{\partial x^2}+\frac{\partial^2 T_f}{\partial y^2}+\frac{\partial^2 T_f}{\partial z^2}\right) \quad (5)$$

2.3 Turbulent model

The turbulent flow was modeled using the realizable viscous model with thermal enhancement near the wall as a swirling flow. This differs from the standard model, where the realizable model has an alternative formula for turbulent viscosity. The modified transport equation for the dissipation rate has been derived from an exact equation for the transport of the mean-square vorticity fluctuation. The equations were as given in (6) and (7) [25].

$$\frac{\partial}{\partial x_j}(\rho k u_j=\frac{\partial}{\partial x_j}[\left(\mu+\frac{\mu_t}{\sigma_k}\right)\frac{\partial k}{\partial x_j}]+G_k+G_b-\rho\varepsilon-Y_M+S_k \quad (6)$$

$$\frac{\partial}{\partial x_j}(\rho\varepsilon u_j=\frac{\partial}{\partial x_j}[\left(\mu+\frac{\mu_t}{\sigma_\varepsilon}\right)\frac{\partial \varepsilon}{\partial x_j}]+\rho C_1 S_\varepsilon-\rho C_2\frac{\varepsilon^2}{k+\sqrt{\vartheta\varepsilon}}+C_1\varepsilon\frac{\varepsilon}{k}C_3 G_b+S_\varepsilon \quad (7)$$

Where $$C_1=Max\left[0.43\frac{\eta}{\eta+5}\right],\eta=S\frac{K}{\varepsilon}\ ,S=\sqrt{2S_{ij}}$$

G_k represents the generation of turbulence kinetic energy due to the mean velocity gradients in these equations. G_b is the generation of turbulence kinetic energy due to buoyancy. Y_m represents the contribution of the fluctuating dilatation in compressible turbulence to the overall dissipation rate. C_2 and $C_1\varepsilon$ are constants. σ_k and σ_ε Are the turbulent Prandtl numbers for k and ε, respectively. S_k and S ε are user-defined source terms. The model constants have been established to ensure that the model performs well for specific canonical flows. The model constants were:

$$C_{1\varepsilon}=1.4, C_1=1.9, \sigma_k=1, \sigma_3=1.2$$

2.4 Data Reduction

Investigating the hydrothermal performance in a tube can be done using the following related expressions:
Equations (8 -14) were important due to the calculation of several parameters [24].

$$f=\frac{\Delta P}{(L/D)(\rho U2/2)} \quad (8)$$

$$\Delta p=\ p_{in}-p_{out} \quad (9)$$

$$\mathrm{Re}=\frac{\rho*u*D_h}{\mu} \quad (10)$$

$$Nu=\frac{h*D}{k} \quad (11)$$

Where h was the heat transfer coefficient (W/M^2 .K), and K was the conductive heat transfer coefficient (Wm/ K)

$$h_{\text{ave}}=\frac{q_f}{A_{\text{Con.}}(T_w-T_b)} \quad (12)$$

Where, $A_{con.}$, the area of convection heat transfer (test tube wall), T_w average temperature of the test tube wall, T_b average fluid temperature and D_h was hydraulic diameter. q_f was the amount of heat gained by the fluid from the pipe's hot walls, which can be calculated using equation (13).

$$q_f=\dot{m}Cp(T_o-T_{in}) \quad (13)$$

Where Cp was the Specific heat capacity of water and ṁ was the mass flow rate (kg /s).
A Performance Evaluation Factor (PEF) was used to check the overall hydrothermal heat enhancement:

$$PEC\ =(\frac{Nu}{Nu_\circ})/(\frac{f}{f_\circ})^{1/3} \quad (14)$$

3 NUMERICAL SIMULATIONS

3.1 Physical modeling

A 3D numerical modeling and conjugate heat transfer simulation was solved with the finite-element method based on the CFD software package ANSYS Fluent 2022 R1, which solves coupled hydrothermal problems like multiphase phenomena. The numerical model consists of an entrance tube connected to a test tube that was assumed to be

completely thermally insulated, in which two types of twisted tapes were inserted into the test tube (normal and modified) with three twisting ratios TR (7.8, 3.9 and 2.6) respectively for each type. Figure 1 shows the test tube, the modified twisted tapes with three twisting ratios, and the entrance tube. Figure 2 shows, in a three-dimensional form, the connection of the twisted tape to the entrance tube. Solid Work program was used to build the numerical structure, and Figure 3 shows the modified twisted tape in the Solid Work program before twisting. Table 1 shows the dimensions that were adopted in building the numerical model.

Table 1. The dimensions in the numerical model

Type	Daimeter D (mm)	Length L (mm)	Width W (mm)	Thickness t (mm)
Test tube	50	1200	-	1.5
Entrance	50	500	-	1.5
Twisted tape	-	1200	38	2

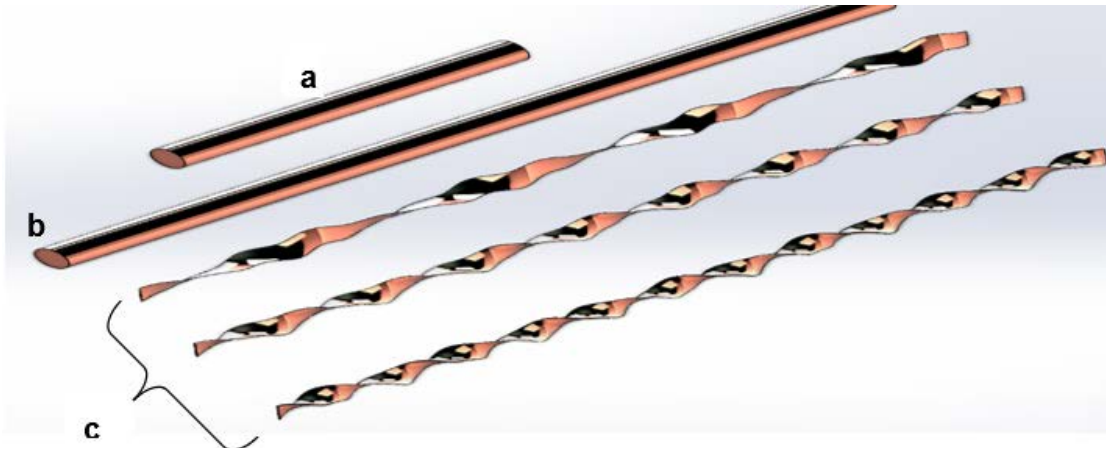

Fig.1. (a) entrance, (b) test tube and (c) modified twisted tapes

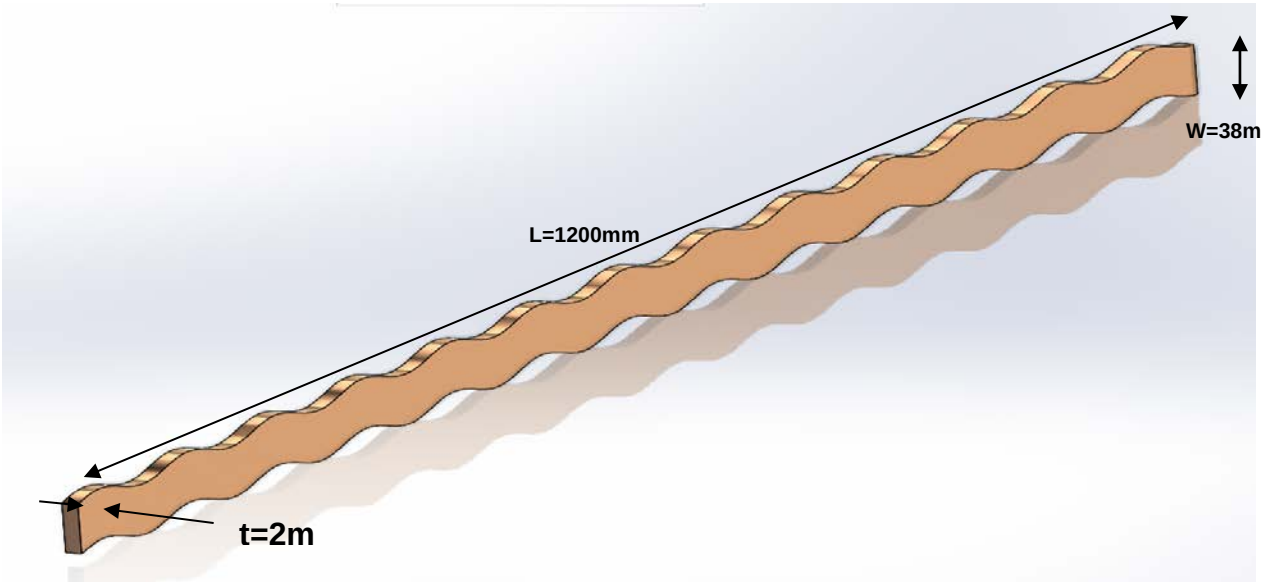

Fig. 2. Modified twisted tape before twisting

3.2 Boundary conditions

At the entrance, the inlet set the inlet velocity with three water flow rate values, and the test tube's exit was set to the outlet pressure. The inlet fluid temperature was 289 K. No slip condition was imposed at twisted tape surfaces and the tube walls. For all-simulation calculation, there are three different constant wall heat fluxes; the walls of the test tube are exposed to heat flux as (2750, 4000,5250) W, respectively. When using numerical calculations, it was verified that changing the wall temperature impacts the tube's heat transfer factor and friction coefficient.

3.3 Grid-independent analysis

The results of any numerical model solved using ANSYS fluent base software are affected by the grid number and mesh type; therefore, the mesh dependency must be checked. Mesh dependency can be achieved by calculating

any result of any variable with the mesh type or number of the node, so calculate the percentage of the errors for two successive iterations. When the error percentage was less, the results must be taken at this range of nodes. In this research, the Nusselt number was taken as the variable parameter, which is affected by the number of elements, and was used to validate the accuracy of numerical solutions. The sweep method grid was used for mesh, as shown in Figure 3 The Nu number's stabilizations were considered a standard for calculation convergence. The mesh dependency testing was shown in Figure 4 to determine whether the choosing mesh was sufficient. Many grid sensitivity tests were performed to ensure that the results were grid-independent, and for this work, 2,350,000 nodes were selected for all the computations.

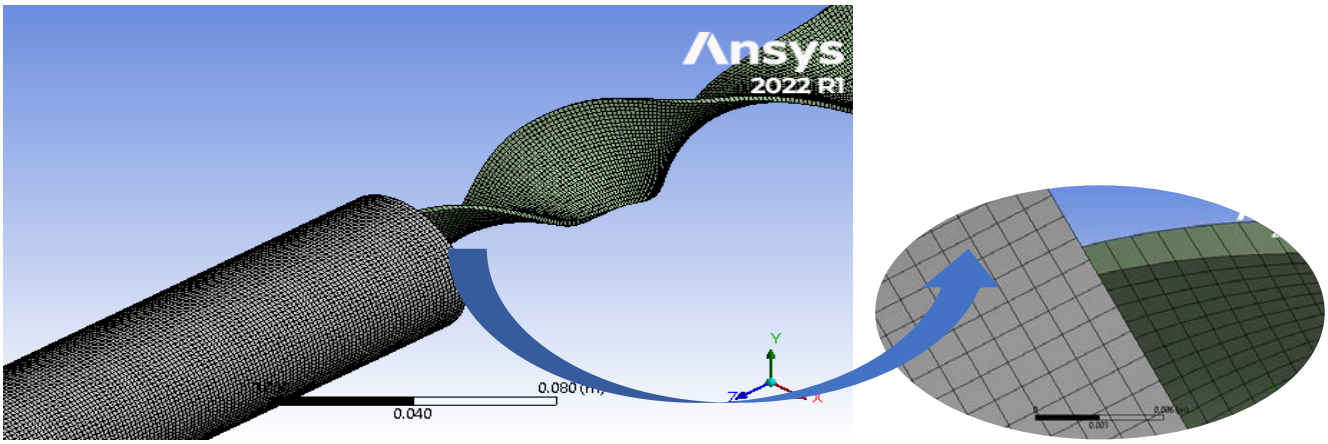

Fig. 3. The mesh with sweep method grid

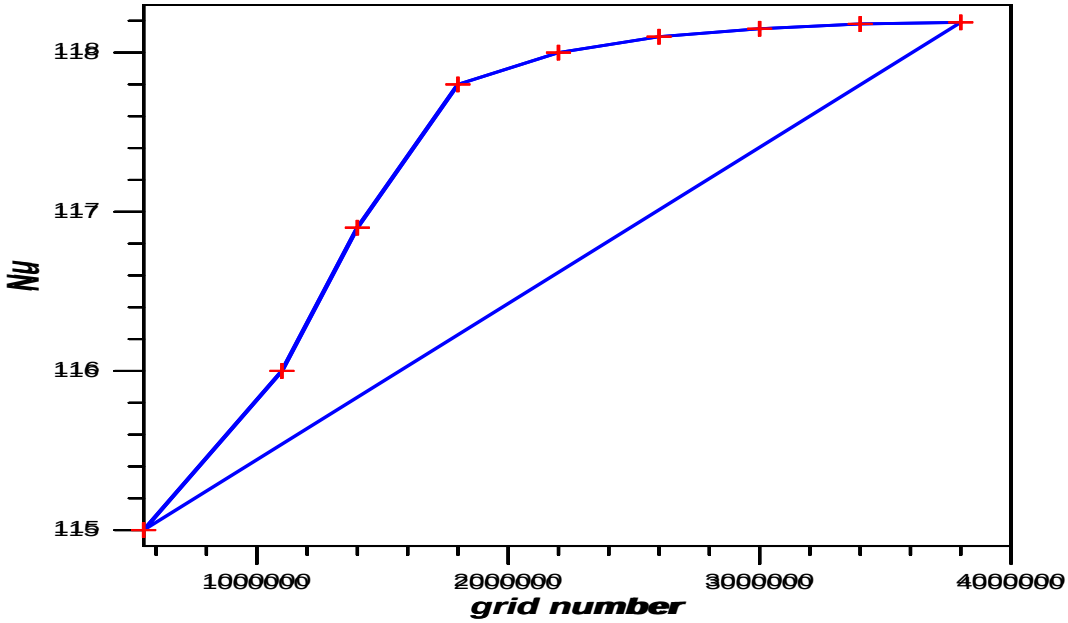

Fig. 4. Mesh independence results using turbulence model (R k – ε EWT) with wall heat flux 5250 W for average Nusselt number for modified twisted tape

3.4 Model Validation

The model of computational fluid dynamics was validated by comparing it with the numerical simulation results obtained by Karrar A. Hammoodi [27] for 3-D smooth channel single-phase flow (water as working fluid) with an intake Reynolds number range of 10000–20000 at a wall temperature of 673 K. The maximum errors of the Nusselt number between the result of the present model and the numerical result obtained from Karrar A. Hammoodi were 1.482%, 1.581%,1.553%,0.688%, 0.872%, and 1.368%. The maximum errors of outlet temperature between the present model results and the numerical results of Karrar A. Hammoodi were 0.25%, 0.5%, 0.6%, 1.2%, 1.1%, and 2%, respectively, corresponding to the Reynolds numbers taken as shown in Figures 5 (a)& (b). It is very clear from the comparison between [38] and the present model that the two curves have the same trend, and this analysis shows that the highest degree of agreement for these outcomes illustrates the reliability of these models in precisely forecasting the flow structure and the properties of heat transfer.

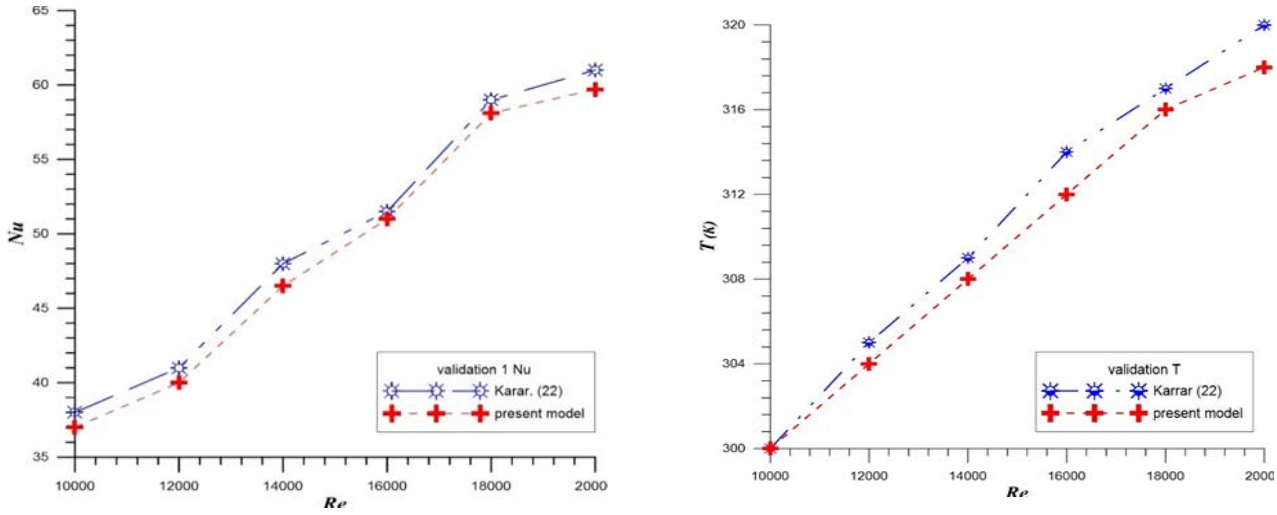

(a) Nu (b) T at otlet

Fig. 5. Validation between the present work and Karrar A. Hammoodi et al. [27] for (a) Nu and (b) outlet temperature

4 RESULTS AND DISCUSSION

For forced convection heat transfer using twisted tape, parameters like tape twist ratio, fluid flow rate, and temperature difference are crucial. The twist ratio enhances turbulence, promoting better mixing and heat transfer. A typical range for the twist ratio might be between 0.5 and 3, while flow rates can vary widely depending on the application, often from 0.1 to 5 m/s. This allows for a comprehensive understanding of how these factors influence heat transfer efficiency.

4.1 Effect of heat flux on Nusselt number

The constant heat flux on the test tube wall was varied from 2750, 4000, and 5250 W to study their effects on average Nu numbers. Fig. 6 (a), (b), and (c) showed the changes for each configuration. The increase in Nu numbers was proportional relatively to the increase in heat flux at the range of the study. In this figure, a pipe without a vortex generator was compared with a pipe using a plain twisted stripe. It was clear that plain twisted stripes obtained the highest Nusselt values. It was indicated in Fig. 7 (c) that there were the highest increases for pipes when using the 2.6 twisted ratio of plain twisted tape at Re 10547 and heat flux at 5250 W, where the Nusselt number reached 146. The lowest value among the three types was in Figure 7 (a), where it reached 80 at a Ronald number of 6500 and a heat flux of 2750 when using a twisted ratio of 7.8. Other than that, the trends of increasing the Nu numbers due to the inlet Re numbers for other models were somewhat similar. Notably, Nu increased by around 30 for 45% when the heat flux increased from 2750 to 5250 W for tubes with plain twisted tape inserts and tubes without twisted tape, respectively. Figures 10 a, b, and c showed the effect of the rate of heat flux on the change in Nusselt values for the modified twisted tape, where noticed that in all Figures a, b, and c, there was a turbulent increase in Nu numbers values when the heat flux rates were increased until reached of the highest Nusselt number value = 152 at the twist ratio of 2.6 at the rate of heat flux was 5250 W. The Reynolds number was 10500, an increase of 1.25 over the lowest Nusselt value, which was 120 at 2750 W and for the same conditions.

4.2 Effect of Re on Nusselt number

As the Reynolds number increases, indicating a transition from laminar to turbulent flow, the flow becomes more chaotic. This turbulence enhances mixing within the fluid, which increases the convective heat transfer coefficient (h). Figures 7 a, b and c show the effect of the Re number on the Nusselt number at constant heat flux for each design by comparing the modified twisted tape with the plain twisted tape, which appears from the figures that the increase in the Nusselt number was directly proportional to the increase in the Re number, and in general the modified twisted tape obtained higher Nusselt number values compared to plain twisted tape. The modified twisted tape with a twist ratio of 2.6 was the best in terms of thermal performance, and the highest value reached was 146 at a heat flux of 5250 W and a Re number of 10540 .The percentage increase reached 1.8, while the plain twisted tape with a twist ratio of 7.8 had the lowest thermal performance, reaching 80 at Re number of 6300 and heat flux at 2750 W.

4.3 Effect of twist ratio on Nusselt number

A higher twist tape ratio increases the intensity of turbulence in the flow. This leads to better fluid mixing, which enhances the heat transfer rate. The twist ratio effecting was studied using different models: tubes with plain stripes inserts, tubes with modified stripes inserts, and twisted tape inserts at twist ratios of 7.8, 3.9, and 2.6, and its effect on the heat transfer rate. As shown in Figure 9, a, b, and c are comparisons of the behavior of the modified twisted tape and the plain twisted tape according to each value of the twist ratio for each shape and each value of the heat

flux and its effect on the Nusselt number. Figures 8 (a), (b), and (c) show the superiority of the modified twisted tape over the plain twisted tape for all twist ratios and all heat flow values because the wavy edge of the modified twisted tape increases the turbulence intensity more which causes an increase in the heat transfer coefficient. In Figure 9 c, the twist ratio of 2.6 for modified twisted tape showed the highest Nusselt value, reaching 152 at a Roland number of 10500 and a heat flux of 5250 W; the percentage increase reached 1.9. In comparison, the twist ratio of 2.6 for plain twisted tape recorded the lowest value of 80 at a Re number of 6500 and a heat flux of 2750 W.

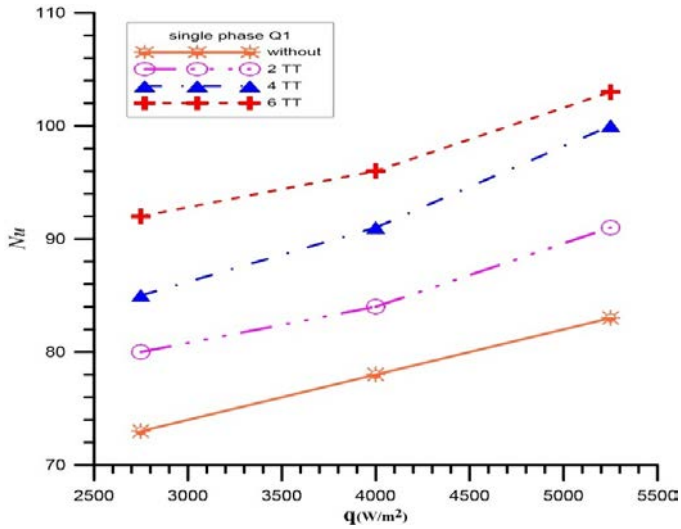

(a) Q_{w1}=15 l/min

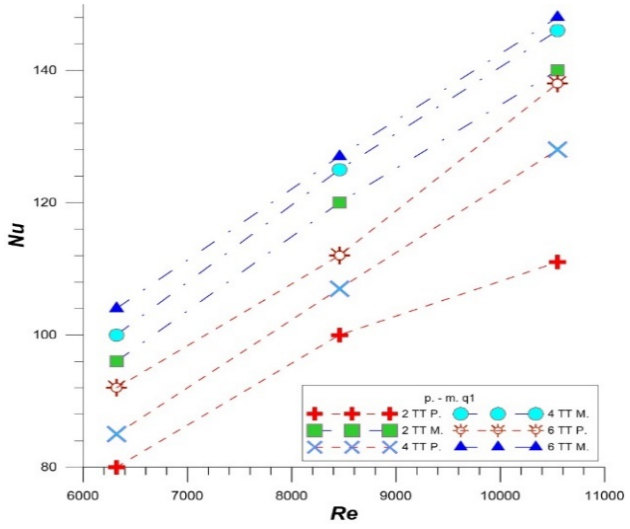

(a) q_1=2750 W

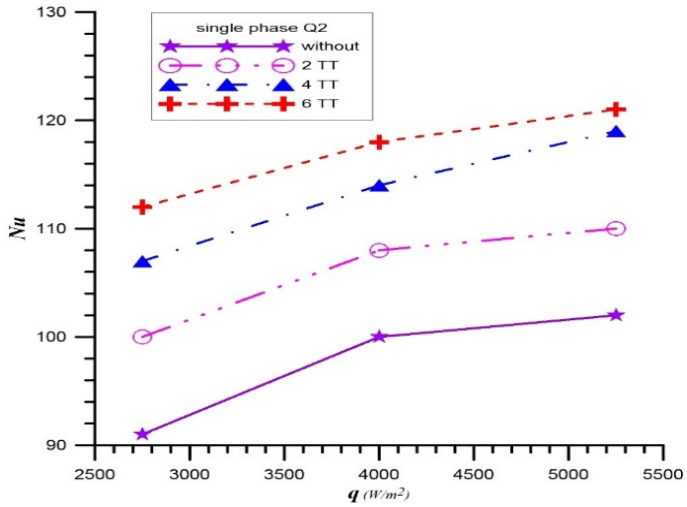

(b) Q_{w2}=20 l/min

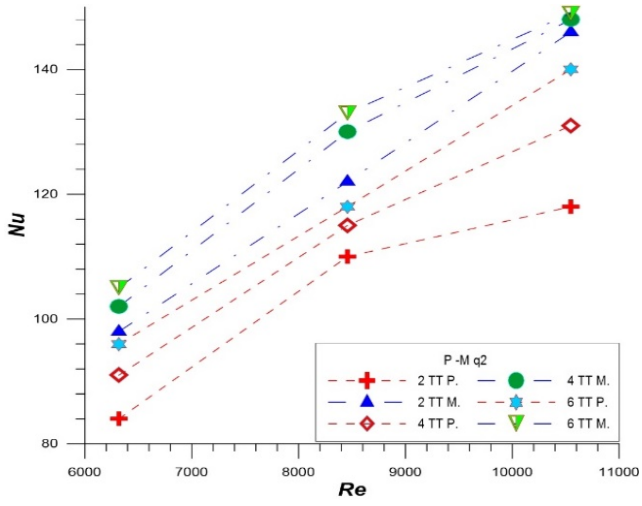

(b) q_2=4000 W

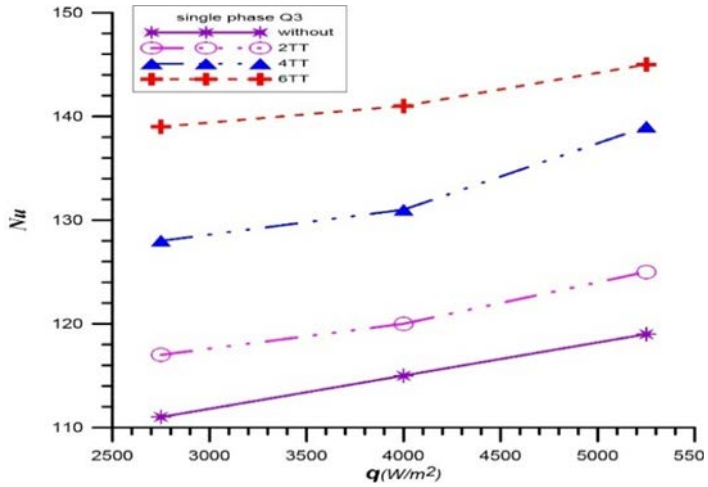

(c) Q_{w3}=25 l/min

Fig. 6. (a), (b) and (c) compares Nu for tubes inserted TT without and plain for different water flow rates

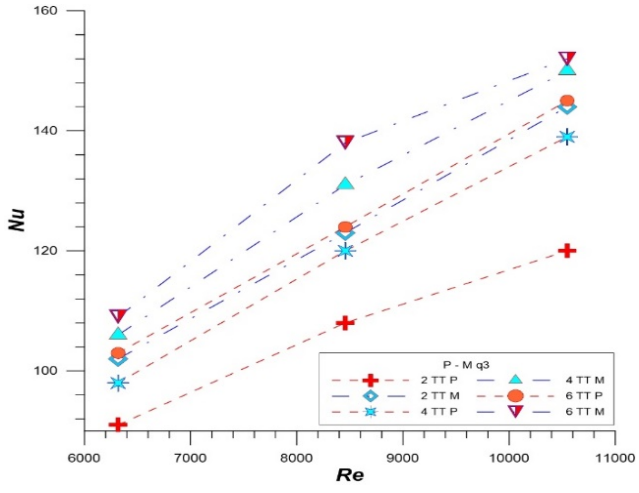

(c) q_3=5250 W

Fig. 7. (a), (b), and (c) compare Nu for tubes inserted TT Plain and modified for different heat fluxes

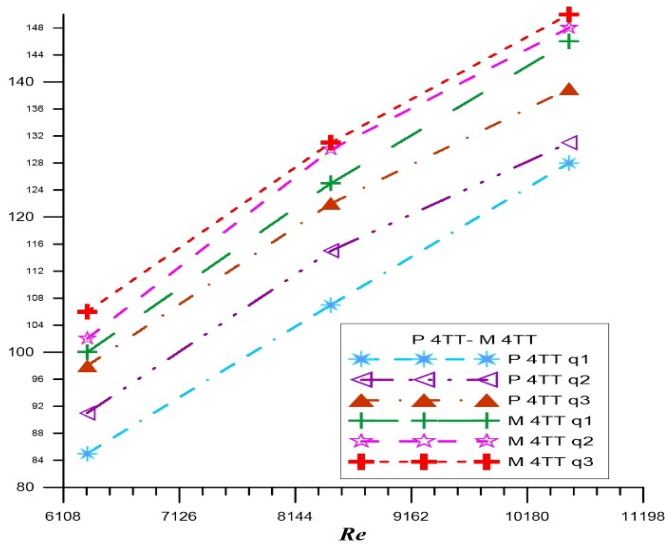

(a) TR=7.8

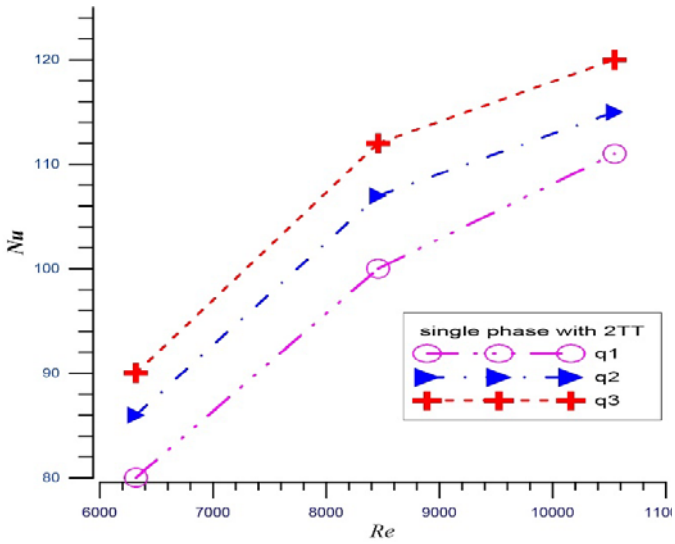

(a) TR=7.8

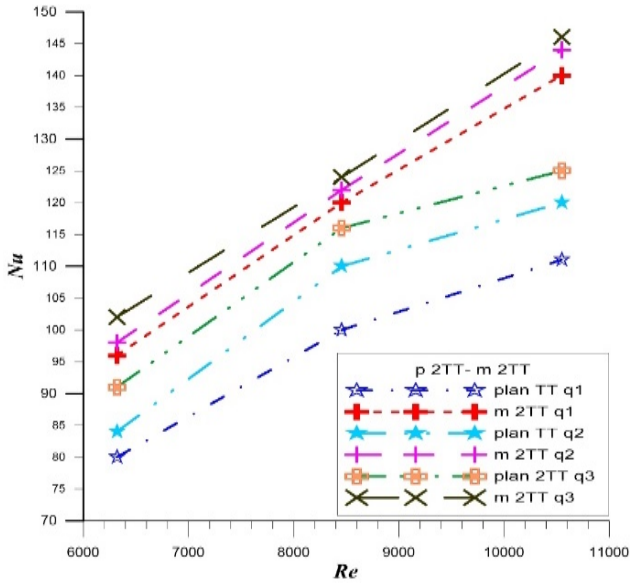

(b) TR2=3.9

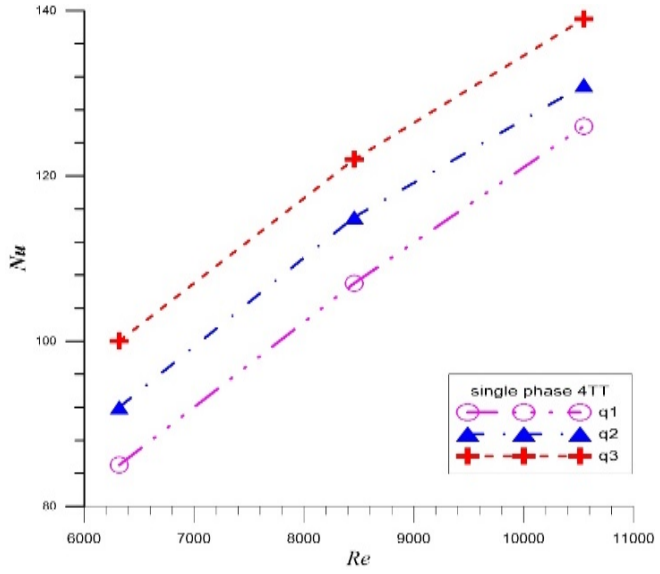

(c) TR2=3.9

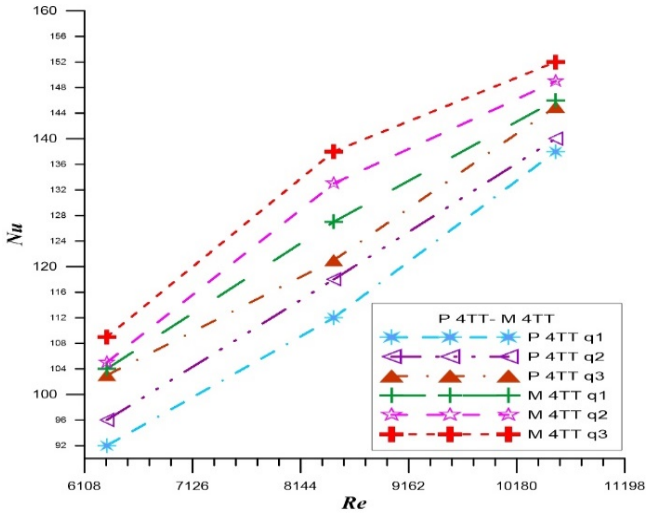

(c) TR3=2.6

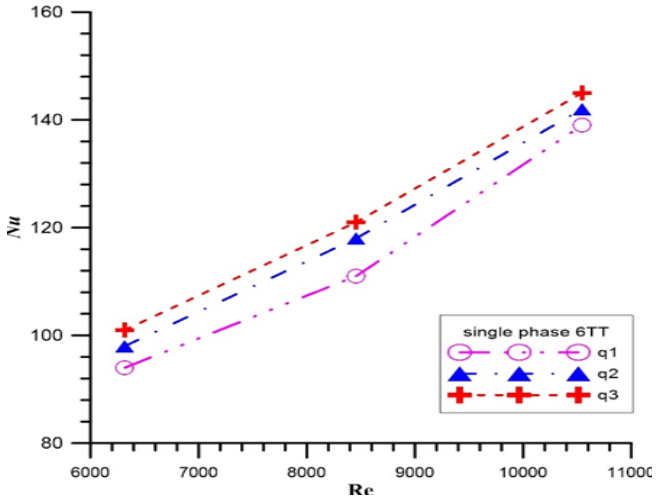

(c) TR3=2.6

Fig. 8. (a), (b), and (c) compare Nu for tubes with 3TR for Plain and modified TT for three heat fluxes

Fig. 9. (a), (b) and (c) compare Nu for modified TT at three heat fluxes

4.4 Effect of water flow rate (Q) on friction factor (f)

Figure (10) (a,b,c) shows the behavior of friction factor at the range of Reynolds number for water flow without twisted tape and with three plain twisted and three modified twisted tape; it can be noted that the lowest value in the friction factor was recorded for flow without a twisted tape because there are no obstacles, while when using the plain twisted tap the friction factor increases and continues to increase by increase the twisted ratio until the highest value was reached at a twisted ratio of 2.6. In contrast, when using modified twisted tape, the friction factor was more than the flow without twisted tape at the same time, less than the value of the plain twisted for all flow rate magnitude, and this is a positive point for the modified twisted tape. In the exact figure, the friction coefficient decreased for all flow values as the water flow rate increased for all types of inserted twisted tapes and all degrees of twisting.

In Figure(11)(a,b,c), it can be seen that the friction coefficient increased when the heat flux along the test tube wall was increased. It can also be noted that for the case flow with a twisted ratio of 2.6 at a Re of 10547, the friction factor increased by 2% with the increase in the rate of heat flux delivery from 2750 W to 5350 W, which resulted in an increase in the friction coefficient as a result of the water's density decreasing as temperature rose.

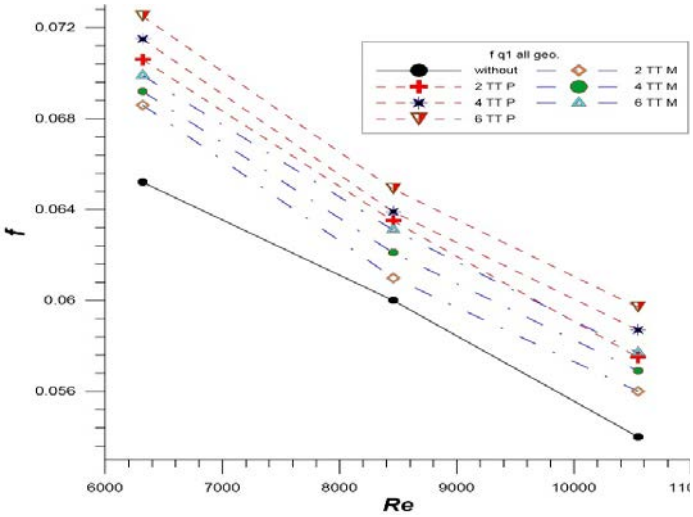

(a) q_1=2750W/m^2

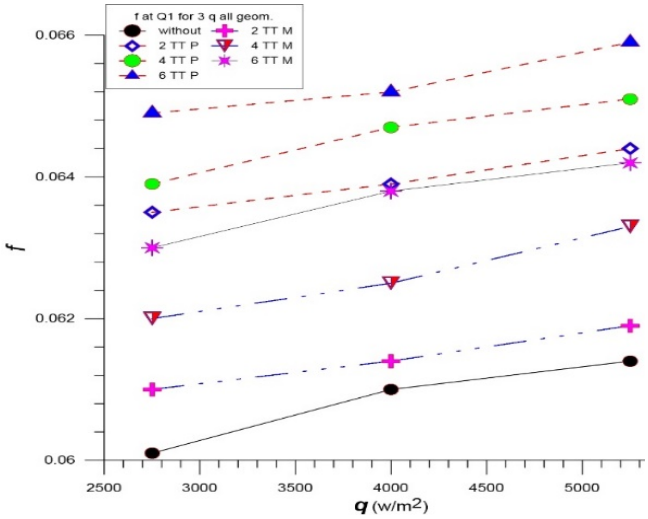

(a) Q_1=15 l/min

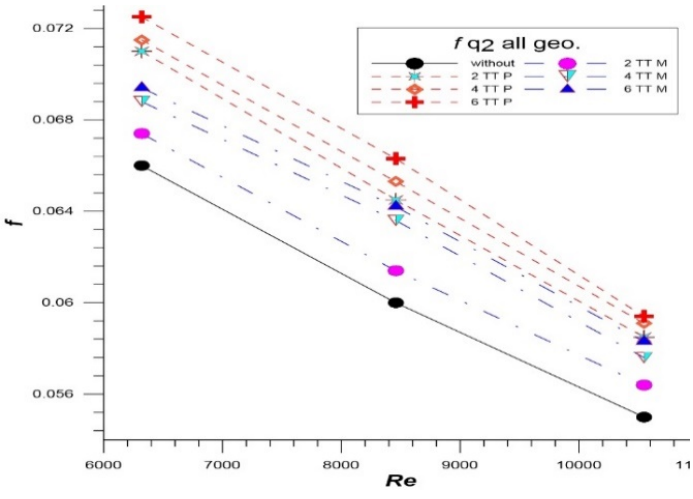

(b) q_2=4000W/m^2

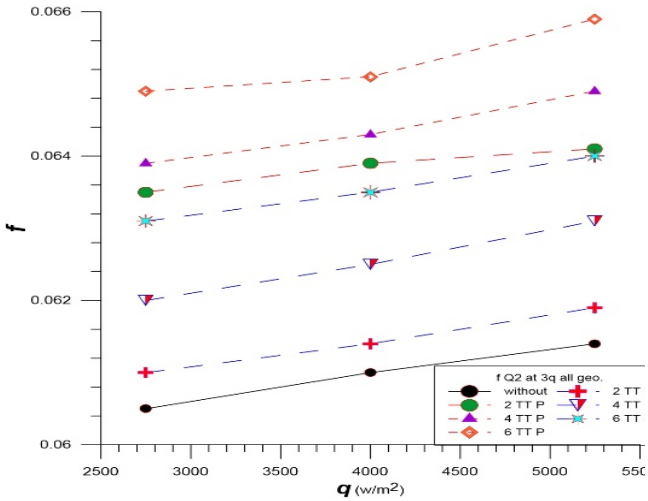

(b) Q_2=20 l/min

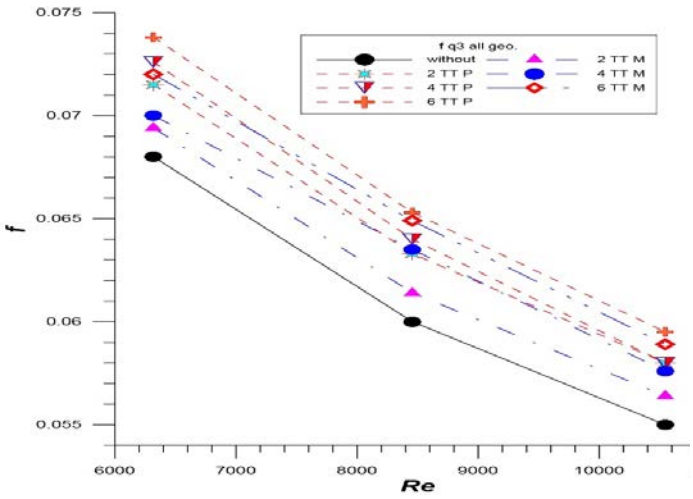

(c) q_3=5250W/m^2

Fig.10 (a), (b) and (c) comparison of *f* for (without, three plain and three modified) twisted tapes

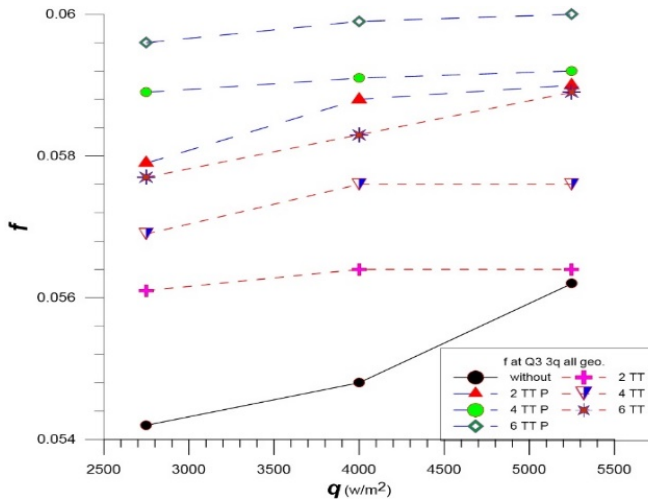

(c) Q_3=25 l/min

Fig.11 (a), (b), and (c) compare *f* at the range of water flow rates

4.5 Velocity distributions

Figures 12 a, b, and c show the streamlines of the turbulent flow of water as a function of velocity at the outlet cross-section of the tube without a twisted tape. It can be noted that the streamlines are few and far apart at a flow rate of 15 l/min and increase as the flow rate increases. At the same time, Figures 13 a, b, and c show the streamlines when using the plain twisted tape, which increases the intensity of the flow lines, and vortices begin to appear due to the presence of the twisted strip, which acts as a vortex generator and generates swirling flow. This intensity and vortices increase as the flow rate increases. Figures 14 a, b, and c were for the tube that contains a modified twisted strip, where the vortices are more apparent. It is more disordered due to the wavy edge of the twisted strip. Figures 15, 16, and 17 (a, b, and c) show the turbulent streamlines through the tubes without a twisted strip, with a plain twisted strip, and with a modified twisted strip at a heat flux of 5250 W. It clearly shows an increase in the intensity of the streamlines with increasing heat flow compared to Figures 15, 16, and 17 (a, b, and c), which were at a heat flux of 2750 W. This was caused by the fluid's decreased density and decreased viscosity as a result of rising temperatures, which increases the flow's tendency to produce vortices.

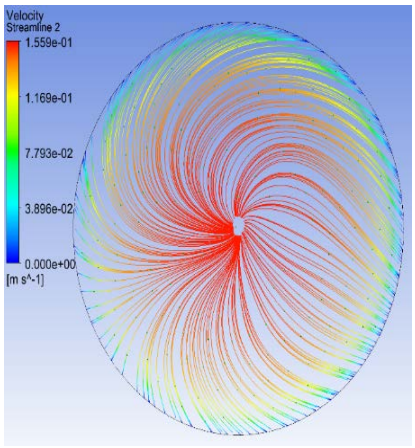

Q=15 l/min

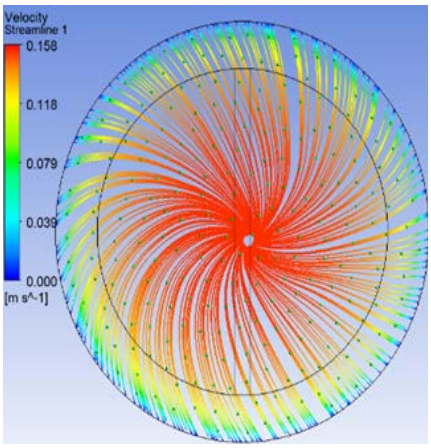

Q=15 l/min

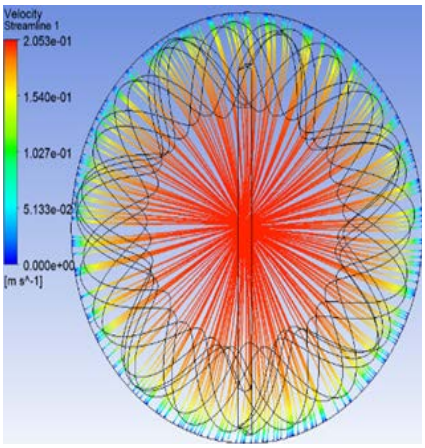

Q=15 l/min

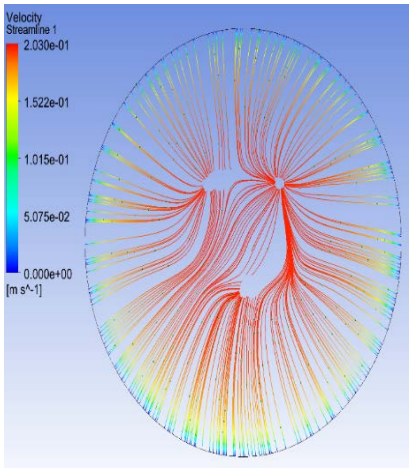

Q=20 l/min

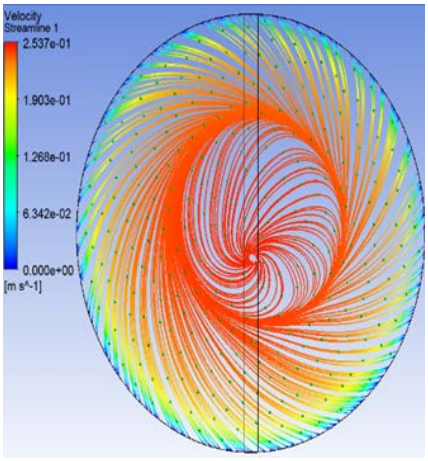

Q=20 l/min

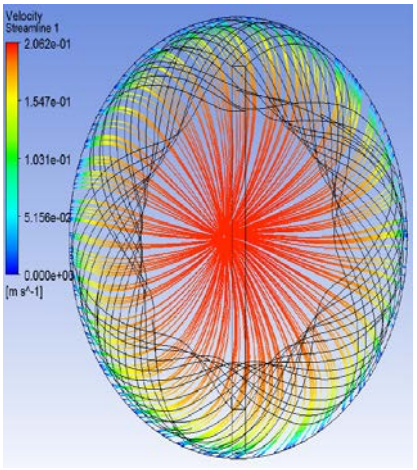

Q=20 l/min

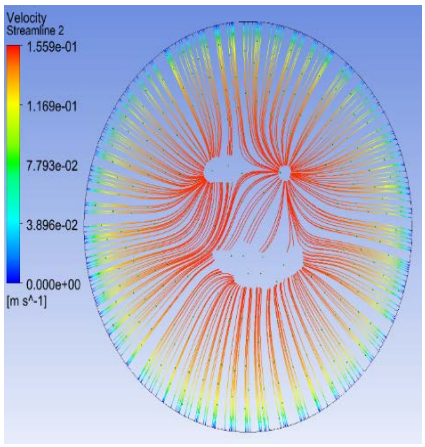

Q= 25 l/min

Fig. 12 (a),(b) and (c) velocity distribution of tube without twisted tape, q1

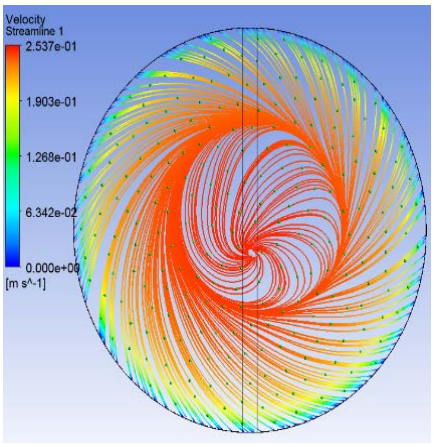

Q=25 l/min

Fig. 13 (a),(b) and (c) velocity distribution of tube with plain twisted tape,q1, TR 7.8

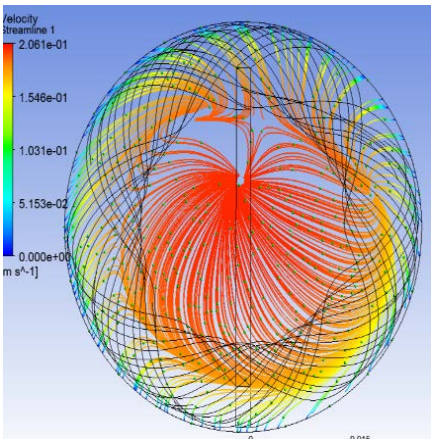

Q=25 l/min

Fig. 14 (a),(b) and (c) velocity distribution of tube with modified twisted tape,q1, TR 7.8

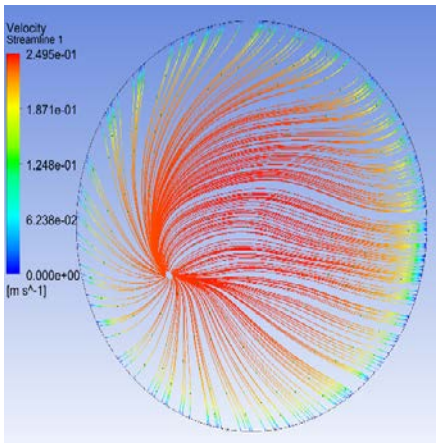

Q=15 l/min

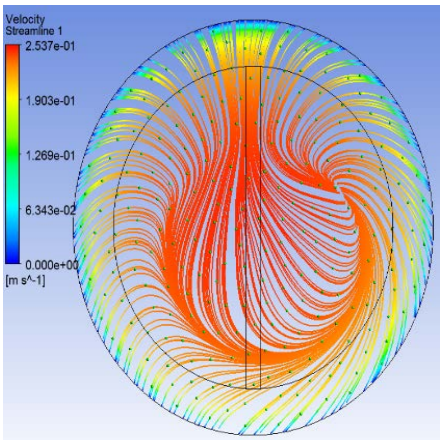

Q=15 l/min

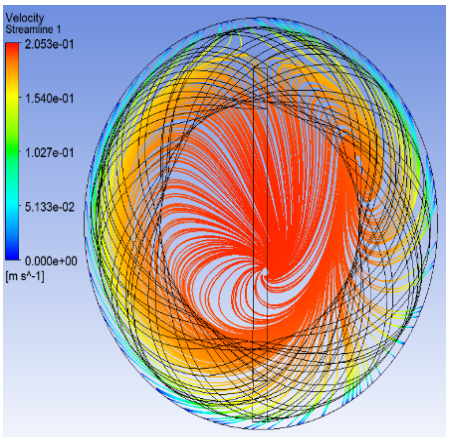

Q=15 l/min

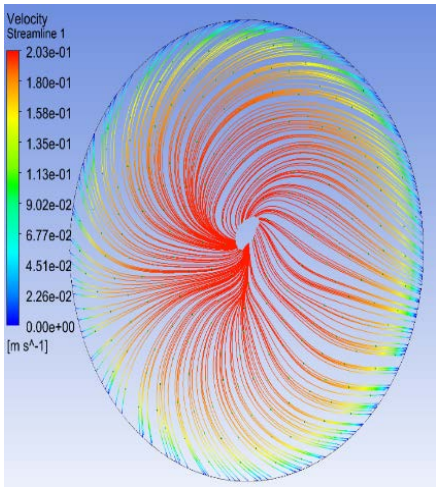

Q=20 l/min

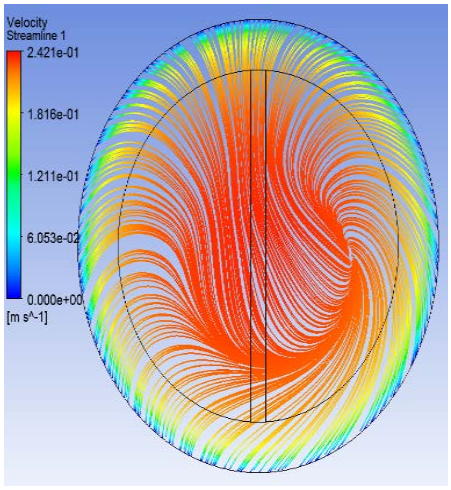

Q=20 l/min

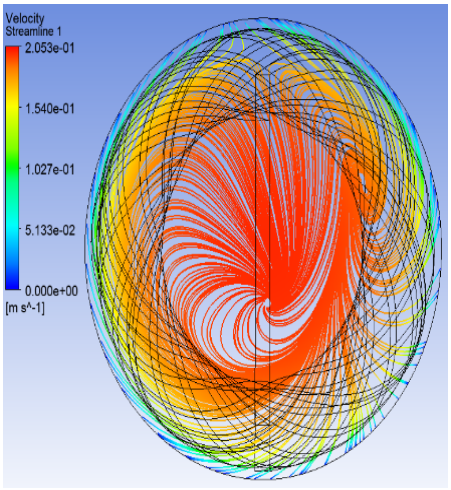

Q=20 l/min

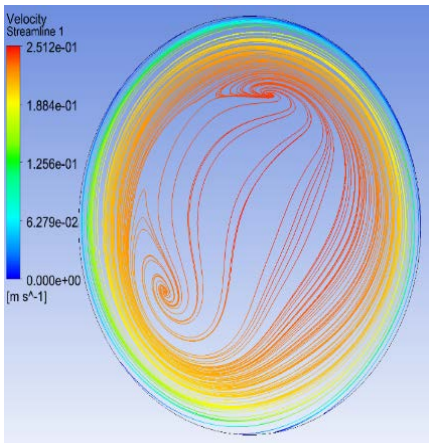

Q=25 l/min

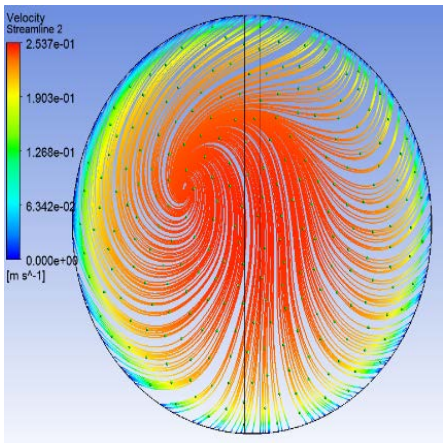

Q=25 l/min

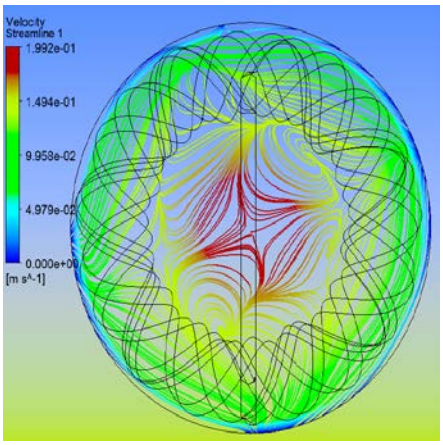

Q=25 l/min

Fig. 15 (a),(b) and (c) velocity distribution of tube without twisted tape insert,q_3

Fig. 16 (a),(b) and (c) velocity distribution of tube with plain twisted tape TR 2.6,q_3

Fig. 17 (a),(b) and (c) velocity distribution of tube with modified twisted tape TR 2.6,q_3

4.6 The Performance Evaluation Factor (PEF) Effecting

An important factor, the performance evaluation factor PEF, was tested to balance the heat transfer enhancement quantity (Nu/Nuo) with pressure losses (f/fo) [37]. Figure 18 (a), (b), and (c) shows the effect of heat flux (q) on PEF at different twisted ratios for plain and modified twisted tape. Can notice that for all shapes a, b, and c, the modified twisted stripe obtained the highest value of the TPF, which reached 1.5 at a heat flux of 2750 W and at a twist ratio of 3.9 at Re 8450, obtaining a higher Nusselt number as well as a lower coefficient of friction for all shapes when compared to the plain twisted tape. It can also be noted that the twist ratio of 4 obtained the highest values for all shapes because the modified twisted tape obtained a higher Nusselt number than the rest. Although the modified twisted tape of twisted ratio 2.6 obtained the highest Nusselt number among all shapes, at the same time, the friction coefficient significantly increased due to the increase in the number of coils, which acts as an obstacle to the flow and, therefore generally decreases the performance evaluation factor. Figures 19 (a), (b), and (c) show the effect of water flow rates (Q) on PEF for plain and modified twisted tape at various twisted ratios. Can notice that for all fingers a, b, and c, the modified twisted tape obtained the highest values of the thermal performance factor when compared with the plain twisted tape because the waving edge of the tape enhancement the heat transfer by generating more turbulent leads to increase the Nusselt number which covered on the increasing friction factor, which led to the PEF reaching its highest value of 1.49 at a water flow rate of 20 l/min and a twist ratio of 3.9 at a heat flux of 2750 W, obtaining a higher Nusselt number as well as a lower friction factor for all shapes. It can also be noted that the twist ratio of 4 obtained the highest values of PEF for all modified models. Although the modified twisted tape of twisted ratio 2.6 obtained the highest Nusselt number among all shapes, at the same time, the friction coefficient significantly increased due to the increase in the number of coils, which acts as an obstacle to the flow and, therefore generally decreases the performance evaluation factor.

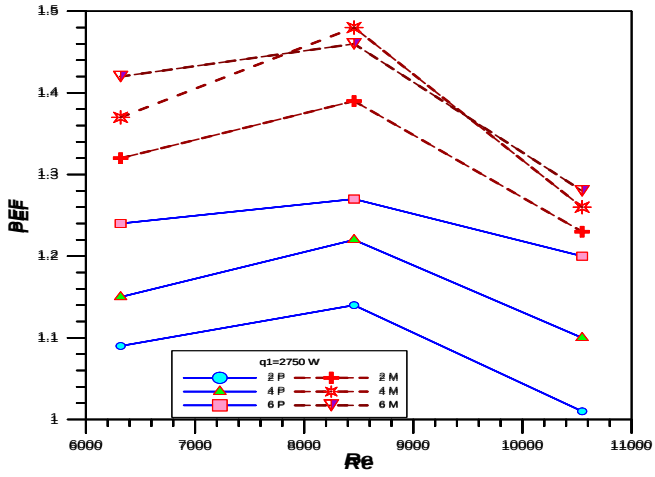

(a) q1=2750 W/m2

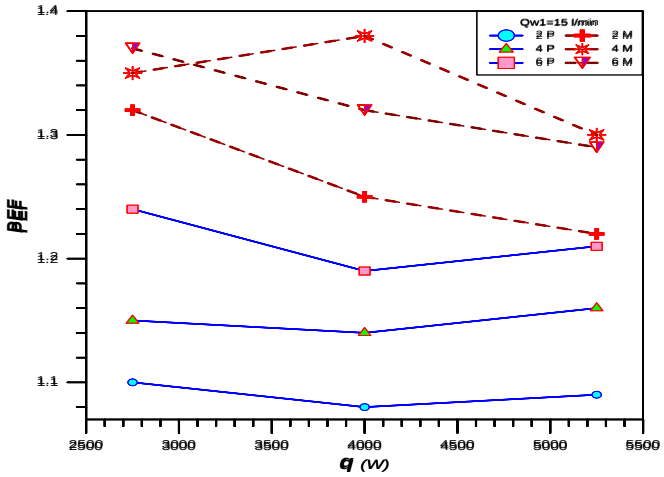

(b) Qw1= 15 l/min

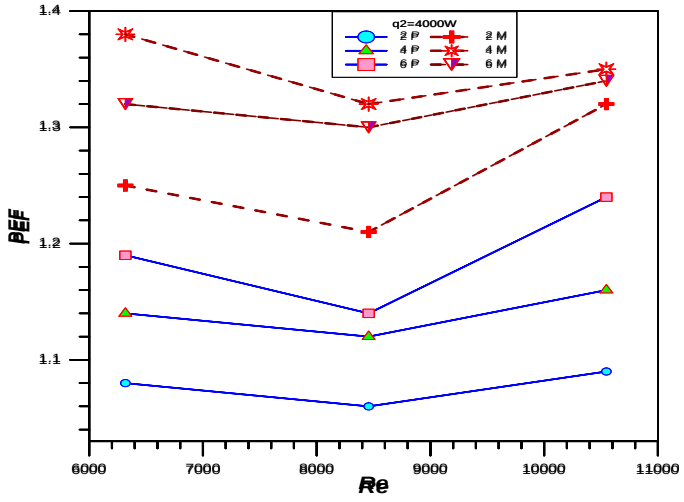

(a) q2=4000 W/m2

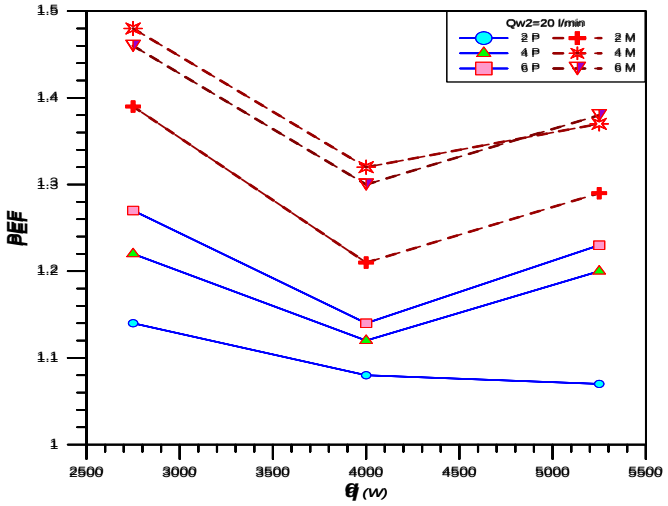

(b) QW2=20 l/min

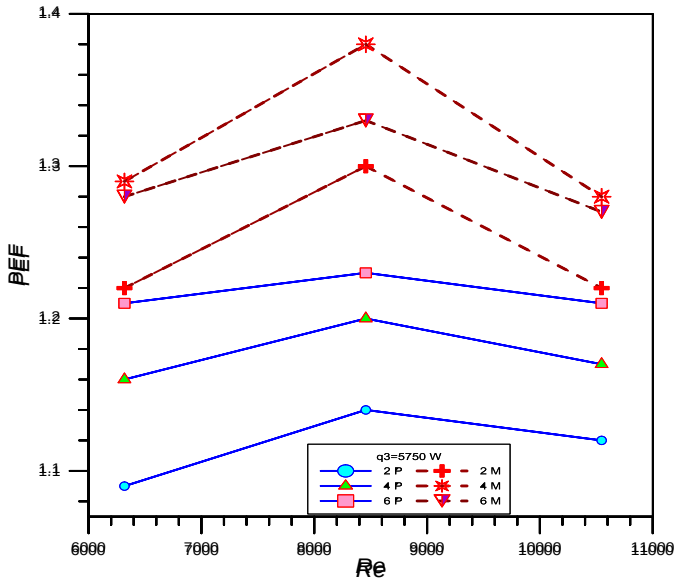

(c) q_3=5250 W/m^2

Fig. 18. (a),(b) and (c) comparison of the PEF for plain and modified twisted tape at three heat fluxes.

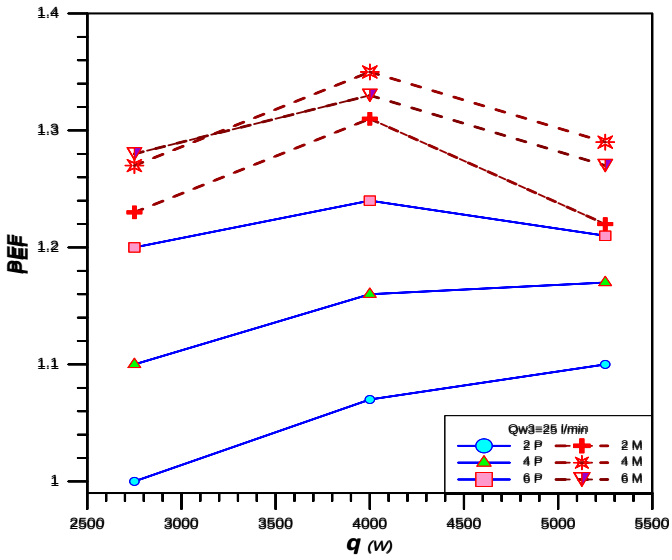

(c) Q_{w3}=25 l/min

Fig. 19. (a), (b) and (c) comparison of the PEF for plain and modified twisted tape for three water flow rates

5 CONCLUSIONS

The present work investigates the heat transfer indicated by Nu, the friction losses indicated by *f*, the Performance Evaluation Factor (PEF) and the velocity distribution of different flow rates and heat fluxes in a vertical tube without and with (plain and modified) twisted tape inserts with a variable twisted ratio. The results showed that:

- When quantities of heat flux and Reynolds numbers increased, heat transfer increased in all cases.
- When using the twisted tape (of both types), the heat transfer was significantly improved, but at the same time, the coefficient of friction also increased.
- There was more enhancement when decreasing the tape's twist ratio in general, where the highest Nu number was 152, obtained when using the modified twisted tape with a twist rate of 2.6.
- The PEF reached the highest 1.5 for modified twisted tape with a twisted ratio of 3.9 at a Reynolds number of 6500 and a heat flux of 5250 W.
- In general, the friction factor increased when twisted tape of all types was inserted and increased as the twisting rate decreased.
- It was observed that the insertion of the twisted strip enhanced the turbulence intensity, increased the generation of vortices, and converted the flow into a swirling flow.

6 REFERENCES

[1] Bahiraei, M., Mazaheri, N., & Hassanzamani, S. M. (2019). Efficacy of a new graphene–platinum nanofluid in tubes fitted with single and twin twisted tapes regarding counter and co-swirling flows for efficient use of energy. International Journal of Mechanical Sciences, 150, 290-303.

[2] Al-Daamee, F.Q. and N.H. Hamza, On the effect of wave amplitude and corrugation profile of certain types of corrugated channels on thermal performance and entropy generation. International Journal of Thermal Sciences, 2025. 207: p. 109354. https://doi.org/10.1016/j.ijthermalsci.2024.109354.

[3] Hamza NH, Abdulkadhim A, Mohsen AM, Abed AM. Analysis of double-diffusive hydrothermal flow in a domestic stack: The effect of side walls patterns. Heat Transfer. 2024; 53: 707-732. https://doi.org/10.1002/htj.22972.

[4] Majhool, A.A., Hamza, N.H. & Jasim, N.M. Spray Interface Drag Modeling Based on the Power-Law Droplet Velocity Using the Moment Theory. J Appl Mech Tech Phy 61, 61–69 (2020). https://doi.org/10.1134/S0021894420010071.

[5] Fatimah Q. Al-Daamee, Naseer H. Hamza, Numerical investigation of thermal and entropy generation characteristics in a sinusoidal corrugated channel under the influence of sinusoidal wall temperature, International Journal of Thermofluids, Volume 22, 2024, 100706, ISSN 2666-2027, https://doi.org/10.1016/j.ijft.2024.100706.

[6] Al-Ali, H. M., & Hamza, N. H. (2023). Numerical and experimental study of the influence of extended surfaces in rectangular channel subjected to constant heat flux. Experimental Heat Transfer, 37(6), 609–627. https://doi.org/10.1080/08916152.2023.2176567.

[7] Yang, D., Khan, T. S., Al-Hajri, E., Ayub, Z. H., & Ayub, A. H. (2019). Geometric optimisation of shell and tube heat exchanger with interstitial twisted tapes outside the tubes applying CFD techniques. Applied Thermal Engineering, 152, 559-572. https://doi.org/10.1016/j.applthermaleng.2019.01.113

[8] Abid Allah H, N., Sh. Alnasur, F., Abdulkadhim, A., Mejbel Abed, I., Mahjoub Said, N., & Abed, A. M. (2024). MHD natural convection in a wavy nanofluid enclosure with an internally corrugated porous cylinder. Journal of Taibah University for Science, 18(1), 2335685. https://doi.org/10.1080/16583655.2024.2335685

[9] Tavakoli, M., & Soufivand, M. R. (2023). Investing entropy generation, PEC, and efficiency of parabolic solar collector containing water/Al2O3− MWCNT hybrid nanofluid in the presence of finned and perforated twisted tape turbulators using a two-phase flow scheme. Engineering Analysis with Boundary Elements, 148, 324-335.

[10] Liaw, K. L., Kurnia, J. C., & Sasmito, A. P. (2021). Turbulent convective heat transfer in a helical tube with twisted tape insert—International Journal of Heat and Mass Transfer, 169, 120918.

[11] Al-Obaidi, A. R., & Chaer, I. (2021). Study the flow characteristics, pressure drop and augmentation of heat performance in a horizontal pipe with and without twisted tape inserts—Case Studies in Thermal Engineering, 25, 100964.

[12] Ju, Y., Zhu, T., Mashayekhi, R., Mohammed, H. I., Khan, A., Talebizadehsardari, P., & Yaïci, W. (2021). Evaluation of multiple semi-twisted tape inserts in a heat exchanger pipe using Al2O3 nanofluid. Nanomaterials, 11(6), 1570.

[13] Arasteh, H., Rahbari, A., Mashayekhi, R., Keshmiri, A., Mahani, R. B., & Talebizadehsardari, P. (2021). Effect of pitch distance of rotational twisted tape on the heat transfer and fluid flow characteristics. International Journal of Thermal Sciences, 170, 106966. https://doi.org/10.1016/j.ijthermalsci.2021.106966

[14] Yadav, A. S., Shrivastava, V., Dwivedi, M. K., & Shukla, O. P. (2021). 3-dimensional CFD simulation and correlation development for circular tube equipped with twisted tape. Materials Today: Proceedings, 47, 2662-2668.

[15] Yang, Z., Liu, X., Cao, X., Gao, Z., & Ding, M. (2020). Numerical analysis of FLiBe laminar convective heat transfer characteristics in tubes fitted with coaxial cross-twisted tape inserts. Frontiers in Energy Research, 8, 178.

[16] Nakhchi, M. E., Hatami, M., & Rahmati, M. (2020). Experimental investigation of heat transfer enhancement of a heat exchanger tube equipped with double-cut twisted tapes. Applied Thermal Engineering, 180, 115863.

[17] Mushatet, K. S., Rishak, Q. A., & Fagr, M. H. (2020). Experimental and numerical investigation of swirling turbulent flow and heat transfer due to the insertion of twisted tapes of new models in a heated tube. Applied Thermal Engineering, 171, 115070.

[18] Nakhchi, M. E., & Esfahani, J. A. (2019). Numerical investigation of rectangular-cut twisted tape insert on performance improvement of heat exchangers. International Journal of Thermal Sciences, 138, 75-83.

[19] Kumar, N. R., Bhramara, P., Kirubeil, A., Sundar, L. S., Singh, M. K., & Sousa, A. C. (2018). Effect of twisted tape inserts on heat transfer, friction factor of Fe3O4 nanofluids flow in a double pipe U-bend heat exchanger. International Communications in Heat and Mass Transfer, 95, 53-62.

[20] Liu, X., Ding, M., Bian, H., Yan, C., & Li, C. (2017, July). Numerical Study on Heat Transfer and Resistance of a Tube Fitted With New Twisted Tapes for Lubricating Oil. In International Conference on Nuclear Engineering (Vol. 57861, p. V008T09A052). American Society of Mechanical Engineers.

[21] Razzaq, A. K. A., & Mushatet, K. S. (2022). Evaluation of the performance of the double tube heat exchanger by using combined twisted tube and nanofluid. International Journal of Mechanical Engineering, 7(1), 6618-6628.

[22] Eiamsa-ard, S., Changcharoen, W., Beigzadeh, R., Eiamsa-ard, P., Wongcharee, K., & Chuwattanakul, V. (2021). Influence of co/counter arrangements of multiple twisted-tape bundles on heat transfer intensification. Chemical Engineering and Processing-Process Intensification, 160, 108304.

[23] Alnasur, Fawzi Sh, et al.(2020) "A Study of the Chemical Properties of Cane as a Biofuel After Thermal Treatment Processes (Tarification)." Journal of Physics: Conference Series. Vol. 1664. No. 1. IOP Publishing,

[24] Kalateh, M. R., Kianifar, A., & Sardarabadi, M. (2022). A three-dimensional numerical study of the effects of various twisted tapes on heat transfer characteristics and flow field in a tube: Experimental validation and multi-objective optimisation methodology. Sustainable Energy Technologies and Assessments, 50, 101798.

[25] Fluent, A. N. S. Y. S. (2011). Ansys fluent theory guide. Ansys Inc., USA, 15317, 724-746.

[26] Hammoodi, K. A., Hasan, H. A., M. H., Basem, A., A. M. (2022). Control of heat transfer in circular channels using oblique, triangular ribs. Results in Engineering, 15, 100471. https://doi.org/10.1016/j.rineng.2022.100471

Paper submitted: 01.06.2024.

Paper accepted: 04.11.2024.